Polymer Journal

REGULAR ARTICLE

Phonon Dispersion and Heat Capacity in Microbial Poly(ε-L-lysine)(M-ε-PL)

By Mahendra SINGH,[1] *Abhishek K.* MISHRA,[2] *Navnit K.* MISRA,[1] *Poonam* TANDON,[3,*] *Ko-Ki* KUNIMOTO,[4] *and V. D.* GUPTA[3]

Microbial poly(ε-L-lysine)(M-ε-PL) is a naturally occurring biomaterial, which is water soluble, biodegradable, edible and non-toxic towards humans and environment. Normal mode analysis including phonon dispersion has been performed to understand completely the vibrational spectra of this polymer. Various characteristic features of the dispersion curves have been reported. The heat capacity is calculated as a function of temperature *via* density-of-states in the range 1–450 K.

KEY WORDS: Microbial Poly(ε-L-lysine) / Density-of-states / Phonon Dispersion / Heat Capacity /

Due to the environmental problems related to the plastic materials, there is an ongoing worldwide research effort to develop biodegradable polymers. Poly(amino acid)s are an important class of biodegradable polymers based on natural amino acids linked by amide bonds.[1] These belong to small group of polyamides that consist of only one type of amino acids linked by amide bonds. They are different from proteins that are polyamides of different amino acids. Poly(ε-L-lysine)(ε-PL) is an unusual cationic, naturally occurring homopolyamide made of L-lysine, having amide linkage between ε-amino and α-carboxyl groups [Figure 1]. Polyaminoacids have been suggested and recently investigated as a potential family of biodegradable polymers with optimum mechanical and thermal properties, as well as processing and susceptibility to degradation.[2,3]

Kushwaha *et al.*[4] were the first to report the chemical synthesis of ε-PL. They discussed the conformational behaviour of the polymer in aqueous solution based on CD spectra. On the basis of mainly pH dependence of CD spectra, they concluded that it assumes a β-sheet conformation in aqueous alkaline solution. At acidic pHs, ε-PL took up an electrostatically expanded conformation due to repulsion of protonated α-amino groups, whereas at elevated pH above pK_a of α-amino group, the conformation changed to antiparallel β-sheet like structure. Shima and Sakai isolated ε-PL from culture filtrate of *Streptomyces albulus* and studied its fermentation conditions and physicochemical properties.[5–8] This microbially produced ε-PL abbreviated as M-ε-PL is a naturally occurring biomaterial, which is water soluble, biodegradable, edible and non-toxic towards humans and environment. It shows antibacterial activities against a large number of microorganisms, due to which it finds application as a preservative for various food products.[9] Other potential applications of this polymer are as emulsifying agent, dietary agent, biodegradable fibers, highly water absorbable hydrogels, drug carriers, anticancer agent enhancer and biochip coatings.[10]

Polymeric systems in general and biopolymers in particular are capable of existing in a variety of conformations. The type of conformation taken up by them dictates almost all their properties. Spectroscopic approach has proved a very powerful diagnostic tool in characterizing their conformation. Several workers[11–15] have studied the molecular structure and conformation of M-ε-PL, which indicate that it assumes a β sheet conformation. For example, Maeda *et al.*[14] recorded FT-IR, FT-Raman and ^{13}C NMR spectra to investigate the conformation of M-ε-PL. FT-IR and FT-Raman spectra indicate that it assumes β-sheet conformation in solid state. ^{13}C NMR suggested that M-ε-PL existed as a mixture of two crystalline forms. Introduction of several CH_2 groups in the backbone of the chain makes it possible to view this polymer as sequential copolymer of polyethylene and poly(α-peptide) type sequences.

Vibrational spectroscopy is an important tool for probing conformation through conformationally sensitive modes of a polymer. In general, the IR absorption, Raman spectra, inelastic neutron scattering (INS) from polymeric systems are very complex and cannot be unraveled without the full knowledge of dispersion curves. One cannot appreciate without it the origin of both symmetry dependent and symmetry independent spectral features. Normal mode analysis helps in precise assignment and identification of spectral features. Further the presence of regions of high density-of-states that appears in all these techniques and play an important role in the thermodynamical behaviour is also dependent on the profile of dispersion curves. The lack of this information in many polymeric systems has been responsible for incomplete understanding of polymeric spectra. Dispersion curves also provide information on the extent of coupling along the chain together with an understanding of the dependence of the frequency of the given mode upon the sequence length of ordered conformation.

[1]Department of Physics, Brahmanand P.G. College, Kanpur 224 008, India
[2]Department of Physics, Amity School of Engineering, Amity University, Noida 201 301, India
[3]Department of Physics, University of Lucknow, Lucknow 226 007, India
[4]Kanazawa University, Kakuma-machi, Kanazawa 920-1192, Japan
*To whom correspondence should be addressed (Tel: +91-522-278-2653, Fax: +91-522-278-2653, E-mail: poonam_tandon@yahoo.co.uk).

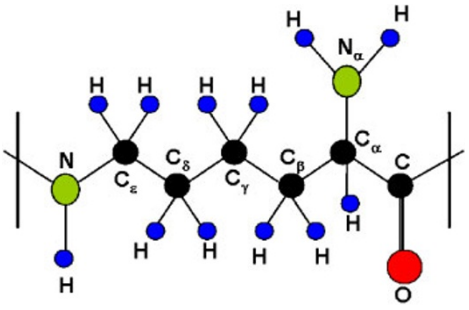

Figure 1. One chemical repeat unit of M-*ε*-PL.

Misra *et al.*[16] reported a detailed dynamical study of helical poly(*α*-L-lysine) but no such work has been reported on M-*ε*-PL. In the present work, we report a comprehensive study of normal mode analysis, phonon dispersion, density-of-states and heat capacity of M-*ε*-PL using Urey-Bradley force field (UBFF). This potential field in addition to valence force field accounts for the non-bonded interactions in the *gem* and *cis* configuration and the tension terms. The density-of-states is used to calculate heat capacity, which enables us to correlate the microscopic behaviour with macroscopic properties. The predictive values of heat capacity are being reported in the temperature range 1–450 K.

THEORY

Calculation of Normal Mode Frequencies

Normal mode calculations for a polymeric chain were carried out using Wilson's GF matrix method[17] as modified by Higgs[18] for an infinite polymeric chain. The vibrational secular equation to be solved is

$$|G(\delta)F(\delta) - \lambda(\delta)I| = 0 \quad 0 \le \delta \le \pi \tag{1}$$

where δ is the phase difference between the modes of adjacent chemical units, $G(\delta)$ is the inverse kinetic energy matrix and $F(\delta)$ is the force field matrix for a certain phase value. The wavenumber $\nu_i(\delta)$ in cm^{-1} are related to eigen values by

$$\lambda_i(\delta) = 4\pi^2 c^2 [\nu_i(\delta)]^2 \tag{2}$$

A plot of $\nu_i(\delta)$ versus δ gives the dispersion curve for the i^{th} mode. The use of the type of force field is generally a matter of one's chemical experience and intuition. In the present work, we have used Urey-Bradley force field as it is more comprehensive than valence force field. The Urey-Bradley takes into account both bonded and non-bonded interactions as well as internal tensions.

Calculation of Heat Capacity

Dispersion curves can be used to calculate the specific heat of a polymeric system. For a one-dimensional system, the density-of-state function or the frequency distribution function expresses the way energy is distributed among the various branches of normal modes in the crystal, is calculated from the relation

$$g(\nu) = \sum (\partial \nu_j / \partial \delta)^{-1}]_{\nu j(\delta)=\nu j} \tag{3}$$

The sum is over all the branches j. Considering a solid as an assembly of harmonic oscillators, the frequency distribution $g(\nu)$ is equivalent to a partition function. The constant volume heat capacity can be calculated using Debye's relation

$$C_v = \sum g(\nu_j) K N_A (h\nu_j/KT)^2 \times [\exp(h\nu_j/KT)/\{\exp(h\nu_j/KT) - 1)\}^2] \tag{4}$$

with $\int g(\nu_i) d\nu_i = 1$.

RESULTS AND DISCUSSION

One residue unit of M-*ε*-PL (Figure 1) contains 21 atoms, which give rise to 63 dispersion curves. The geometry of the chain was obtained by molecular modeling techniques and minimization of conformational energy. The structural parameters thus obtained are given in Table I. Initially the force constants were transferred from poly(*ε*-caprolactone) (PCL),[19] *β* poly(L-valine)[20] and poly(*α*-L-lysine)[16] and later modified to give the "best fit" to the observed spectra of Maeda *et al.*[14] The "best-fitted" force constants are given in Table II. The assignments were made on the basis of potential energy distribution (PED), band profile, line intensities and the presence/absence of similar groups in an identical environment. The vibrational frequencies have been calculated for the values of δ ranging from 0 to π in steps of 0.05π. The optically active modes correspond to those at $\delta = 0$ and $\delta = \pi$. The assignments of all modes along with percentage PED are given in Table III.

Table I. Structural Parameters of M-*ε*-PL

Parameters	Values
Bond Lengths	
All C-H Bonds	1.08 Å
All N-H Bonds	1.00 Å
Aliphatic C-C bonds (Except C_α-C = 1.53 Å)	1.54 Å
C=O Bond	1.24 Å
C_α-N_α, N-C_ε Bonds	1.47 Å
C=N Bond	1.32 Å
Bond Angles	
All $\angle C_\alpha$'s, $\angle C_\beta$'s, $\angle C_\gamma$'s, $\angle C_\delta$'s, $\angle C_\varepsilon$'s	109.47°
$\angle$H-N-C_ε, $\angle$N-C-C_α	114.00°
$\angle$O-C-C_α	121.00°
$\angle$C-N-C_ε	123.00°
$\angle$H-N_α-C_α	120.00°
Dihedral Angles	
χ (C_γ-C_δ-C_ε-N)	180.00°
χ (C_β-C_γ-C_δ-C_ε)	180.00°
χ (C_α-C_β-C_γ-C_δ)	180.00°
χ (C-C_α-C_β-C_γ)	180.00°
χ (H-N-C_ε-C_δ)	0.00°
χ (H-N_α-C_α-C_β)	0.00°

Table II. Internal coordinates and force constants for M-ε-PL (mydn/Å)

Internal Coordinates	Force Constants	Internal Coordinates	Force Constants
ν (N-C_ε)	3.000	φ (C_γ-C_β-H)	0.405(0.220)
ν (C_ε-C_δ)	3.350	φ (H-C_β-C_α)	0.460(0.230)
ν (C_δ-C_γ)	3.250	φ (C_γ-C_β-C_α)	0.425(0.500)
ν (C_γ-C_β)	3.150	φ (H-C_β-H)	0.360(0.365)
ν (C_β-C_α)	3.100	φ (C_β-C_α-H)	0.480(0.215)
ν (C_α-C)	2.000	φ (C_β-C_α-N_α)	0.105(0.390)
ν (C=N)	5.600	φ (H-C_α-C)	0.440(0.215)
ν (C_ε-H)	3.920	φ (N_α-C_α-C)	0.130(0.500)
ν (C_δ-H)	4.160	φ (H-C_α-N_α)	0.300(0.800)
ν (C_γ-H)	4.160	φ (C_β-C_α-C)	0.750(0.500)
ν (C_β-H)	4.160	φ (C_α-N_α-H)	0.500(0.600)
ν (C_α-H)	4.163	φ (H-N_α-H)	0.225(0.355)
ν (C_α-N_α)	2.050	φ (C_α-C=O)	0.890(0.900)
ν (N_α-H)	5.840	φ (O=C=N)	0.910(0.900)
ν (C=O)	7.670	φ (C_α-C=N)	0.585(0.600)
ν (N-H)	5.530	φ (C_α=N-H)	0.345(0.520)
φ (N-C_ε-H)	0.230(0.800)	φ (H-N-C_ε)	0.310(0.520)
φ (H-C_ε-C_δ)	0.395(0.220)	φ (C=N-C_ε)	0.440(0.540)
φ (N-C_ε-C_δ)	0.460(0.600)	ω (C=O)	0.500
φ (H-C_ε-H)	0.350(0.360)	ω (N-H)	0.135
φ (C_ε-C_δ-H)	0.429(0.220)	ω (N_α-H)	0.0241
φ (H-C_δ-C_γ)	0.432(0.230)	τ (C_ε-C_δ)	0.041
φ (C_ε-C_δ-C_γ)	0.450(0.600)	τ (C_δ-C_γ)	0.009
φ (H-C_δ-H)	0.360(0.365)	τ (C_γ-C_β)	0.009
φ (C_δ-C_γ-H)	0.405(0.220)	τ (C_β-C_α)	0.011
φ (H-C_γ-C_β)	0.405(0.230)	τ (C_α-C)	0.010
φ (C_δ-C_γ-C_β)	0.476(0.600)	τ (C=N)	0.095
φ (H-C_γ-H)	0.360(0.365)	τ (C_α-N_α)	0.010
		τ (N-C_ε)	0.011

Note: 1. ν, φ, ω and τ denote stretch, angle bend, wag and torsion respectively.
2. Non-bonded force constants are given in parentheses.

Since the spectra below $200\,cm^{-1}$ are not available hence exact fitting of the force constants related to this region could not be carried out. However in the near infrared region, the calculated frequencies depend on both bonded as well as non-bonded interactions and if they generate the best values in this region then it is expected that in the low frequency region as well, they would yield good results because the non-bonded interactions play dominant role in this region as well. Dispersion curves are plotted in Figure 3(a) for the modes below $400\,cm^{-1}$, because the modes above this are either non dispersive or show very little dispersion. Heat capacity is obtained from the dispersion curves *via* density-of-states. Normal mode frequencies are broadly classified under amide modes, methylene modes, NH_2 group modes and other modes.

Amide Modes

The amide linkage is one of the most fundamental and wide spread chemical linkages in nature. Amide groups of polypeptides are strong chromophores in IR absorption, and these groups give rise to strong characteristic bands (Amide A, I to VII), thus amide modes play a vital role in the vibrational dynamics of polypeptides and polyamides. These modes along with other modes have been used for structural diagnosis. On the basis of such diagnostic correlations, secondary structural compositions are estimated in proteins as well. A comparison of the amide modes of M-ε-PL with those of other β sheet polypeptides is given in Table IV. The minor differences between different amide modes are due to the presence of different chemical groups in between amide groups and number of intervening CH_2 groups that affect the long range interaction and side chain involved in the motion. For example in PG I, the amide group is flanked by only one CH_2 group while in M-ε-PL, it is sandwiched between four CH_2 groups and a NH_2CH group. Since amide bands are affected by the dipole-dipole interaction between neighbouring amide groups, their frequencies and intensities are sensitive to the chain conformation.

The amide A band arising from N-H stretching is characteristic of its functional group and because of its being highly localized, it is not sensitive to the chain conformation and side chain structure. This mode is highly sensitive to the strength of N-H···O=C hydrogen bond. We have calculated amide A mode at $3322\,cm^{-1}$ corresponding to the observed peak at $3329/3320$ in cm^{-1} in IR/Raman spectra.[14] It should be noted that this frequency is somewhat more than those in other β polypeptides (Table IV). The force constant of N-H stretch in this case is more, which is consistent with weaker hydrogen bond in the pleated sheet structure as compared to the rippled sheet. Amide I mode has significant contribution from C=O and C-N stretches. This localized mode is calculated at $1639\,cm^{-1}$ at the zone centre and is in agreement with the observed band at $1639/1633\,cm^{-1}$ in IR/Raman spectra.[14] This mode reflects the hydrogen bond strength due to the presence of C=O stretch contributions. It is sensitive to backbone conformation.

Amide II is predominantly an N-H in plane bending mode. It is calculated at $1528\,cm^{-1}$ and assigned to the peak observed at $1540/1523\,cm^{-1}$ (IR/Raman).[14] This agrees well with the amide II modes in other β sheet structures such as β-PLV, β-PALS, β-PG I and β-PLS[20–23] [Table IV].

Amide III is a combination of N-H in plane bend and C-N stretch as in amide II but in opposite phase. The frequency of this mode does not solely depend on the main chain conformation. Side chain structure also plays important role.[24] This mode has been calculated at $1279\,cm^{-1}$ at $\delta = 0$ and assigned to the peak observed at $1280\,cm^{-1}$ in the observed Raman spectra.[14]

Amide IV vibration is associated with the in plane bending of C=O band. This mode calculated at $549\,cm^{-1}$ (at $\delta = 0$) is assigned to the peak appearing at the same value in the observed IR/Raman spectra. This mode is quite sensitive to molecular geometry.

Amide V and VI modes are mainly asymmetric out of plane wag of N-H and C=O bonds respectively. These vibrational modes calculated at 714 and $643\,cm^{-1}$ respectively at the zone centre match well with the observed peaks at $711\,cm^{-1}$ (IR) and $649/645\,cm^{-1}$ in IR/Raman spectra.[14] However, it should be mentioned that amide V and VI are not pure modes. These are mixed up with amide VII mode which is τ(C=N).

Table III. Normal modes and their dispersion in M-ε-PL

Cal. Freq.	Obs. Freq.* IR	Obs. Freq.* Raman	Assignment ($\delta = 0$) PED (%)	Cal. Freq.	Obs. Freq.* IR	Obs. Freq.* Raman	Assignment ($\delta = \pi$) PED (%)
3417	3414	—	ν[N_α-H](99)	3417	3414		ν[N_α-H](99)
3387	3386	3385	ν[N_α-H](99)	3387	3386	3385	ν[N_α-H](99)
3322	3329	3320	ν[N-H](99) (Amide A)	3335	3329	3320	ν[N-H](99)
2941	2936	2933	ν[C_α-H](92)	2941	2936	2933	ν[C_α-H](91)
2940	2936	2933	ν[C_ε-H](85)+ν[C_δ-H](11)	2940	2936	2933	ν[C_ε-H](85)+ν[C_δ-H](11)
2935	2936	2933	ν[C_γ-H](49)+ν[C_β-H](24) +ν[C_δ-H](15)+ν[C_ε-H](8)	2935	2936	2933	ν[C_γ-H](49)+ν[C_β-H](24) +ν[C_δ-H](15)+ν[C_ε-H](8)
2929	2936	2933	ν[C_δ-H](47)+ν[C_β-H](46)	2929	2936	2933	ν[C_δ-H](47)+ν[C_β-H](46)
2925	2936	2933	ν[C_γ-H](47)+ν[C_δ-H](27)+ν[C_β-H](24)	2925	2936	2933	ν[C_γ-H](47)+ν[C_δ-H](27)+ν[C_β-H](24)
2858	2858	2853	ν[C_ε-H](94)+ν[C_δ-H](5)	2858	2858	2853	ν[C_ε-H](94)+ν[C_δ-H](5)
2854	2858	2853	ν[C_γ-H](51)+ν[C_β-H](28)+ν[C_δ-H](18)	2854	2858	2853	ν[C_γ-H](51)+ν[C_β-H](29)+ν[C_δ-H](18)
2851	2858	2853	ν[C_δ-H](49)+ν[C_β-H](48)	2851	2858	2853	ν[C_δ-H](49)+ν[C_β-H](47)
2848	2858	2853	ν[C_γ-H](48)+ν[C_δ-H](27)+ν[C_β-H](25)	2848	2858	2853	ν[C_γ-H](48)+ν[C_δ-H](27)+ν[C_β-H](24)
1639	1639	1633	ν[C=O](48)+ν[C=N](26) (Amide I)	1685	—	—	ν[C=N](37)+φ[H-N-C_ε](16)+ φ[C=N-H](15)+ν[N-C_ε](14)+ν[C=O](6)
1624	1639	1633	φ[C_α-N_α-H](46)+φ[H-N_α-H](41)	1631	1639	1633	ν[C=O](29)+φ[C_α-N_α-H](22) +φ[H-N_α-H](19)+φ[C=N-H](7)
1528	1540	1523	φ[C=N-H](31)+φ[H-N-C_ε](30) +ν[C=N](15)+ν[N-C_ε](6) (Amide II)	1621	1639	1633	φ[C_α-N_α-H](28)+ν[C=O](24) +φ[H-N_α-H](24)+φ[C=N-H](6)
1460	1461	—	φ[H-C_β-H](31)+φ[H-C_δ-H](22) +φ[H-C_γ-H](20)+φ[H-C_β-C_α](7)	1460	1461	—	φ[H-C_β-H](31)+φ[H-C_δ-H](22)+ φ[H-C_γ-H](20)+φ[H-C_β-C_α](7)
1455	1461	—	φ[H-C_δ-H](38)+φ[H-C_β-H](32) +φ[H-C_δ-C_γ](5)+φ[H-C_β-C_α](5)	1455	1461	—	φ[H-C_δ-H](32)+φ[H-C_β-H](29)+ φ[H-C_ε-H](14)
1442	1440	1437	φ[H-C_γ-H](42)+φ[H-C_ε-H](20) +φ[H-C_β-H](9)	1447	1440	1437	φ[H-C_ε-H](54)+φ[N-C_ε-H](13)+ φ[H-C_δ-H](7)+φ[H-C_γ-H](7)+ φ[H-C_β-H](6)
1439	1440	1437	φ[H-C_ε-H](40)+φ[H-C_δ-H](13) +φ[H-C_γ-H](13)+φ[N-C_ε-H](11)	1441	1440	1437	φ[H-C_γ-H](49)+φ[H-C_δ-H](15)+ φ[H-C_β-H](8)+φ[C_δ-C_γ-H](5)
1401	—	—	φ[C_α-N_α-H](25)+ν[C_β-C_α](18) +φ[C_β-C_α-H](13)+φ[H-C_α-N_α](11)	1401	—	—	φ[C_α-N_α-H](26)+ν[C_β-C_α](18)+ φ[C_β-C_α-H](14)+φ[H-C_α-N_α](12)+ φ[C_γ-C_β-H](6)
1380	1376		ν[C_ε-C_δ](18)+ν[C_δ-C_γ](17)+ φ[H-C_δ-C_γ](15)+φ[C_ε-C_δ-H](15)+ φ[N-C_ε-H](6)+φ[H-C_γ-C_β](6)+ φ[C_δ-C_γ-H](6)+[H-C_ε-C_δ](5)	1382	1376	—	ν[C_δ-C_γ](17)+ν[C_ε-C_δ](16) +φ[H-C_δ-C_γ](13)+φ[C_ε-C_δ-H](13) +φ[H-C_γ-C_β](7)+φ[C_δ-C_γ-H](6)
1345	1341	1353	φ[C_γ-C_β-H](14)+ν[C_γ-C_β](13) +φ[H-C_β-C_α](13)+φ[H-C_α-N_α](13) +φ[N-C_ε-H](7)	1341	1341	1353	φ[H-C_α-N_α](24)+φ[C_γ-C_β-H](13)+ φ[H-C_β-C_α](12)+ν[C_γ-C_β](10)+ ν[C_ε-C_δ](5)
1317	1319	1304	φ[H-C_α-N_α](30)+φ[H-C_α-C](15)+ ν[C_α-C](12)	1304	1319	1304	φ[H-C_α-N_α](25)+φ[H-C_α-C](17)+ φ[C_α-N_α-H](14)+φ[N-C_ε-H](8)+ φ[H-C_ε-C_δ](7)
1279	1280	—	ν[C=N](14)+φ[C_α-N_α-H](13) +φ[H-N-C_ε](10) (Amide III)	1291	—	—	φ[H-N-C_ε](10)+φ[N-C_ε-H](10)+ ν[C_α-C](9)+φ[C_ε-C_δ-H](8)+ φ[H-C_δ-C_γ](8)+ν[C=N](8)+ φ[O=C=N](7)
1267	1264	—	φ[N-C_ε-H](21)+φ[H-C_ε-C_δ](20) +φ[H-C_β-C_α](7)+φ[C_γ-C_β-H](7)	1250	—	1255	φ[C_α-N_α-H](14)+φ[H-C_ε-C_δ](12)+ φ[N-C_ε-H](11)+ν[C=N](9) +ν[C=O](8)+φ[H-N-C_ε](7) +φ[C=N-H](7)
1235	1228	—	φ[N-C_ε-H](59)+φ[H-C_ε-C_δ](17) +φ[H-C_δ-C_γ](10)	1235	1228	—	φ[N-C_ε-H](59)+φ[H-C_ε-C_δ](17)+ φ[H-C_δ-C_γ](10)

Continued on the next page.

Continued.

Cal. Freq.	Obs. Freq.* IR	Obs. Freq.* Raman	Assignment ($\delta = 0$) PED (%)	Cal. Freq.	Obs. Freq.* IR	Obs. Freq.* Raman	Assignment ($\delta = \pi$) PED (%)
1224	1228	—	φ[C_α-N_α-H](16)+φ[H-C_γ-C_β](15) +φ[C_δ-C_γ-H](13)+φ[C_ε-C_δ-H](10) +φ[C_β-C_α-H](9)	1222	1228	—	φ[H-C_γ-C_β](19)+φ[C_δ-C_γ-H](17)+ φ[C_ε-C_δ-H](11)+φ[H-C_δ-C_γ](10)+ φ[C_α-N_α-H](7)+φ[C_β-C_α-H](7)+ φ[H-C_β-C_α](7)
1201	—	1200	φ[C_β-C_α-H](28)+φ[H-C_α-C](24)+ φ[C_α-N_α-H](13)+φ[H-C_β-C_α](7)+ φ[C_δ-C_γ-H](6)	1202	—	1200	φ[C_β-C_α-H](31)+φ[H-C_α-C](25)+ φ[C_α-N_α-H](16)+φ[H-C_β-C_α](6)+ φ[C_γ-C_β-H](6)
1166	1171	1162	φ[H-C_β-C_α](38)+φ[C_γ-C_β-H](28) +φ[H-C_δ-C_γ](9)	1167	1171	1162	φ[H-C_β-C_α](38)+φ[C_γ-C_β-H](28)+ φ[H-C_δ-C_γ](10)+φ[C_ε-C_δ-H](7)+ ν[C_α-N_α](6)
1150	—	1140	φ[C_ε-C_δ-H](32)+φ[H-C_δ-C_γ](25) +φ[H-C_β-C_α](10)+[H-C_ε-C_δ](8)	1149	—	1140	φ[C_ε-C_δ-H](32)+φ[H-C_δ-C_γ](24)+ φ[H-C_β-C_α](11)+φ[H-C_γ-C_β](8)+ φ[H-C_ε-C_δ](8)
1120	1123	1122	φ[C_δ-C_γ-H](40)+φ[H-C_γ-C_β](38) +φ[H-C_δ-C_γ](6)	1119	1123	1122	φ[C_δ-C_γ-H](41)+φ[H-C_γ-C_β](39)+ φ[H-C_δ-C_γ](7)
1104	1095	—	ν[N-C_ε](45)+ν[C_β-C_α](6)	1070	1064	1066	ν[C_α-N_α](27)+ν[C_β-C_α](26) +φ[C_β-C_α-C](7)+φ[C_γ-C_β-H](6)
1057	1064	1066	ν[C_α-N_α](27)+ν[C_β-C_α](18) +ν[N-C_ε](16)+ν[C_α-C](8)	1054			ν[N-C_ε](28)+ν[C_δ-C_γ](10) +φ[N-C_ε-C_δ](9)+φ[C_ε-C_δ-C_γ](8) +ν[C=N](6)+ν[C_ε-C_δ](5)
1027	1040	1037	ν[C_δ-C_γ](31)+ν[C_ε-C_δ](18) +φ[C_ε-C_δ-C_γ](8)+φ[C_δ-C_γ-C_β](5)	1009			ν[N-C_ε](26)+ν[C_δ-C_γ](19) +ν[C_ε-C_δ](15)+ν[C_α-N_α](7)+ν[C_α-C](7)
995	1001	1010	ν[C_ε-C_δ](29)+ν[C_γ-C_β](27)+ν[C_δ-C_γ](7) +φ[H-C_ε-C_δ](6)+φ[C_γ-C_β-H](5)	998	1001	1010	ν[C_γ-C_β](30)+ν[C_ε-C_δ](30) +ν[C_δ-C_γ](6)+φ[C_γ-C_β-H](6) +φ[H-C_ε-C_δ](5)
972	972	—	ν[C_γ-C_β](21)+ν[C_δ-C_γ](8)+ φ[H-C_γ-C_β](8)+φ[C_ε-C_δ-H](7)+ φ[C_γ-C_β-H](6)+φ[C_δ-C_γ-H](6)	971	972	—	ν[C_δ-C_γ](22)+ν[C_γ-C_β](17) +φ[H-C_γ-C_β](9)+φ[C_δ-C_γ-H](8) +ν[C_α-N_α](6)+φ[C_ε-C_δ-H](5)
961	—	956	φ[H-C_γ-C_β](11)+φ[C_ε-C_δ-H](11) +ν[C_γ-C_β](10)+φ[H-C_ε-C_δ](10) +φ[H-C_δ-C_γ](10)	958	—	956	φ[C_ε-C_δ-H](12)+φ[H-C_γ-C_β](11)+ φ[H-C_δ-C_γ](10)+φ[H-C_ε-C_δ](9)+ ν[C_γ-C_β](9)+φ[C_δ-C_γ-H](8) +φ[H-C_β-C_α](8)+φ[C_γ-C_β-H](7)
933	—	933	ν[C_α-C](21)+ν[C_β-C_α](10) +ν[C_α-N_α](8)+ν[C_δ-C_γ](8)	937	—	933	ν[C_α-C](23)+ν[C_β-C_α](10)+ν[C=O](7)+ ν[C=N](7)+φ[O=C=N](6)
894	881	—	ν[C_α-N_α](15)+φ[C_γ-C_β-H](10) +φ[H-C_ε-C_δ](9)+ν[C_α-C](8) +ν[C_β-C_α](8)+φ[H-C_δ-C_γ](6)	908	914	—	ν[C_α-N_α](15)+φ[H-C_ε-C_δ](10)+ φ[C_γ-C_β-H](10)+ν[C_β-C_α](7)+ ν[C_α-C](7)
845	—	851	φ[H-C_ε-C_δ](27)+φ[H-C_β-C_α](11)+ φ[C_δ-C_γ-H](11)+ν[C_α-N_α](10) +φ[N-C_ε-H](7)+φ[C_γ-C_β-H](6)	844	—	851	φ[H-C_ε-C_δ](24)+ν[C_α-N_α](16)+ φ[H-C_β-C_α](11)+φ[C_δ-C_γ-H](9)+ φ[N-C_ε-H](7)+φ[C_γ-C_β-H](5)
811	831	—	φ[C_ε-C_δ-H](26)+φ[H-C_δ-C_γ](13)+ τ[C_ε-C_δ](13)+φ[H-C_ε-C_δ](12)+ φ[C_γ-C_β-H](8)	811	831	—	φ[C_ε-C_δ-H](27)+τ[C_ε-C_δ](14)+ φ[H-C_ε-C_δ](14)+φ[H-C_δ-C_γ](13)+ φ[C_γ-C_β-H](7)+φ[H-C_β-C_α](7)
772	768	758	ω[N-H](23)+ω[C=O](17)+τ[C=N](8)	762	768	758	ω[N-H](26)+ω[C=O](18)+τ[C=N](12)
734	—	730	φ[H-C_γ-C_β](22)+φ[C_δ-C_γ-H](19) +φ[C_γ-C_β-H](15)+ω[N-H](10)	741	—	730	φ[H-C_γ-C_β](25)+φ[C_δ-C_γ-H](2)+ φ[C_γ-C_β-H](17)+ω[N-H](8)+ φ[H-C_β-C_α](8)
714	713	—	ω[N-H](21)+τ[C=N](16) +ν[C_α-C](9)+ν[C_α-N_α](7) (Amide V+VII)	711	713	—	ω[N-H](19)+τ[C=N](16)+ν[C_α-C](7) +ν[C_α-N_α](6)+φ[O=C=N](6)+ φ[C_α-C=O](5)
643	649	645	ω[C=O](53)+τ[C=N](13) (Amide VI)	642	649	645	ω[C=O](52)+τ[C=N](13)+ν[C_α-N_α](7)

Continued on the next page.

Continued.

Cal. Freq.	Obs. Freq.* IR	Obs. Freq.* Raman	Assignment ($\delta = 0$) PED (%)	Cal. Freq.	Obs. Freq.* IR	Obs. Freq.* Raman	Assignment ($\delta = \pi$) PED (%)
549	549	550	$\varphi[C_\alpha\text{-}C{=}N](17)+\varphi[C_\delta\text{-}C_\gamma\text{-}C_\beta](15)$ $+\varphi[C_\varepsilon\text{-}C_\delta\text{-}C_\gamma](11)+\varphi[C_\alpha\text{-}C{=}O](11)$ $+\varphi[C_\beta\text{-}C_\alpha\text{-}C](7)$ (Amide IV)	538	549	550	$\varphi[C_\alpha\text{-}C{=}N](18)+\varphi[N\text{-}C_\varepsilon\text{-}C_\delta](14)+$ $\varphi[C_\gamma\text{-}C_\beta\text{-}C_\alpha](13)+\varphi[C_\delta\text{-}C_\gamma\text{-}C_\beta](11)+$ $\varphi[C_\alpha\text{-}C{=}O](10)+\varphi[C_\varepsilon\text{-}C_\delta\text{-}C_\gamma](6)$
489	493	493	$\omega[N_\alpha\text{-}H](74)+\tau[C_\alpha\text{-}N_\alpha](15)$	488	493	493	$\omega[N_\alpha\text{-}H](74)+\tau[C_\alpha\text{-}N_\alpha](15)$
440	—	431	$\varphi[N\text{-}C_\varepsilon\text{-}C_\delta](21)+\varphi[C_\gamma\text{-}C_\beta\text{-}C_\alpha](19)+$ $\varphi[C_\varepsilon\text{-}C_\delta\text{-}C_\gamma](17)+\varphi[C_\delta\text{-}C_\gamma\text{-}C_\beta](10)$	430	—	431	$\varphi[C_\varepsilon\text{-}C_\delta\text{-}C_\gamma](26)+\varphi[C_\delta\text{-}C_\gamma\text{-}C_\beta](21)$ $+\varphi[C_\alpha\text{-}C{=}O](10)+\varphi[C{=}N\text{-}C_\varepsilon](8)$ $+\varphi[O{=}C{=}N](7)+\varphi[C_\beta\text{-}C_\alpha\text{-}C](7)$
382	—	391	$\varphi[N\text{-}C_\varepsilon\text{-}C_\delta](18)+\varphi[C_\delta\text{-}C_\gamma\text{-}C_\beta](14)$ $+\varphi[C_\varepsilon\text{-}C_\delta\text{-}C_\gamma](11)+\varphi[C_\gamma\text{-}C_\beta\text{-}C_\alpha](11)$ $+\varphi[C_\alpha\text{-}C{=}N](10)$	341	—	329	$\varphi[C_\beta\text{-}C_\alpha\text{-}N_\alpha](20)+\varphi[H\text{-}C_\alpha\text{-}C](9)$ $+\tau[C{=}N](8)+\varphi[H\text{-}C_\alpha\text{-}N_\alpha](8)+$ $\tau[C_\varepsilon\text{-}C_\delta](7)+\varphi[C_\beta\text{-}C_\alpha\text{-}H](7)+$ $\varphi[N_\alpha\text{-}C_\alpha\text{-}C](7)+\omega[N\text{-}H](6)$
334	—	330	$\varphi[C_\beta\text{-}C_\alpha\text{-}N_\alpha](14)+\varphi[H\text{-}C_\alpha\text{-}C](10)$ $+\varphi[H\text{-}C_\alpha\text{-}N_\alpha](9)+\varphi[N_\alpha\text{-}C_\alpha\text{-}C](9)$ $+\tau[C{=}N](8)+\varphi[C_\beta\text{-}C_\alpha\text{-}H](7)$	314	—	—	$\nu[N\text{-}C_\varepsilon](12)+\varphi[N\text{-}C_\varepsilon\text{-}C_\delta](11)+$ $\varphi[N_\alpha\text{-}C_\alpha\text{-}C](9)+\nu[C{=}N](8)+$ $\nu[C_\alpha\text{-}C](7)+\tau[C_\alpha\text{-}N_\alpha](6)$
300	—	—	$\tau[C_\alpha\text{-}N_\alpha](68)+\omega[N_\alpha\text{-}H](14)$	299	—	—	$\tau[C_\alpha\text{-}N_\alpha](73)+\omega[N_\alpha\text{-}H](18)$
287	—	281	$\varphi[C_\beta\text{-}C_\alpha\text{-}C](19)+\varphi[C{=}N\text{-}C_\varepsilon](14)$ $+\tau[C_\alpha\text{-}N_\alpha](7)+\varphi[C_\delta\text{-}C_\gamma\text{-}C_\beta](7)$ $+\varphi[C_\alpha\text{-}C{=}O](7)+\varphi[N_\alpha\text{-}C_\alpha\text{-}C](7)$	288	—	281	$\varphi[C_\beta\text{-}C_\alpha\text{-}N_\alpha](19)+\varphi[C_\gamma\text{-}C_\beta\text{-}C_\alpha](17)+$ $\varphi[N\text{-}C_\varepsilon\text{-}C_\delta](11)+\varphi[N_\alpha\text{-}C_\alpha\text{-}C](10)+$ $\nu[C_\alpha\text{-}C](7)+\varphi[C_\beta\text{-}C_\alpha\text{-}C](6)$
256	—	245	$\tau[C_\varepsilon\text{-}C_\delta](32)+\varphi[C_\beta\text{-}C_\alpha\text{-}N_\alpha](15)+$ $\tau[C_\gamma\text{-}C_\beta](7)+\tau[C{=}N](7)$	245	—	245	$\tau[C_\varepsilon\text{-}C_\delta](33)+\tau[C{=}N](7)$ $+\omega[C{=}O](7)+\tau[C_\beta\text{-}C_\alpha](5)$
200	—	207	$\varphi[N_\alpha\text{-}C_\alpha\text{-}C](41)+\varphi[C_\beta\text{-}C_\alpha\text{-}N_\alpha](23)$ $+\tau[C_\varepsilon\text{-}C_\delta](7)$	210	—	215	$\varphi[C_\delta\text{-}C_\gamma\text{-}C_\beta](24)+\varphi[C{=}N\text{-}C_\varepsilon](14)+$ $\varphi[C_\beta\text{-}C_\alpha\text{-}N_\alpha](10)+\varphi[N_\alpha\text{-}C_\alpha\text{-}C](8)+$ $\varphi[N\text{-}C_\varepsilon\text{-}C_\delta](5)$
140	—	—	$\tau[C_\delta\text{-}C_\gamma](42)+\tau[N\text{-}C_\varepsilon](28)$ $+\tau[C_\beta\text{-}C_\alpha](18)$	173	—	—	$\varphi[C_\beta\text{-}C_\alpha\text{-}C](29)+\varphi[C_\varepsilon\text{-}C_\delta\text{-}C_\gamma](18)$ $+\varphi[N_\alpha\text{-}C_\alpha\text{-}C](16)+\varphi[C_\alpha\text{-}C{=}O](7)+$ $\varphi[C_\alpha\text{-}C{=}N](6)$
125	—	—	$\tau[C{=}N](22)+\tau[C_\gamma\text{-}C_\beta](18)+\tau[C_\beta\text{-}C_\alpha](16)$ $+\tau[N\text{-}C_\varepsilon](12)+\omega[N\text{-}H](12)+\tau[C_\varepsilon\text{-}C_\delta](7)$	158	—	—	$\varphi[C_\gamma\text{-}C_\beta\text{-}C_\alpha](13)+\varphi[C{=}N\text{-}C_\varepsilon](10)+$ $\tau[C_\delta\text{-}C_\gamma](9)+\tau[C_\gamma\text{-}C_\beta](7)+$ $\varphi[N\text{-}C_\varepsilon\text{-}C_\delta](6)+\tau[N\text{-}C_\varepsilon](6)$
100	—	—	$\tau[C_\alpha\text{-}C](43)+\tau[N\text{-}C_\varepsilon](20)$ $+\tau[C_\beta\text{-}C_\alpha](13)+\tau[C_\gamma\text{-}C_\beta](11)$	137	—	—	$\tau[N\text{-}C_\varepsilon](28)+\tau[C_\delta\text{-}C_\gamma](24)+$ $\varphi[C_\beta\text{-}C_\alpha\text{-}N_\alpha](10)+\varphi[C_\gamma\text{-}C_\beta\text{-}C_\alpha](7)$
56	—	—	$\varphi[C_\varepsilon\text{-}C_\delta\text{-}C_\gamma](28)+\varphi[C{=}N\text{-}C_\varepsilon](18)+$ $\varphi[N\text{-}C_\varepsilon\text{-}C_\delta](12)+\varphi[C_\gamma\text{-}C_\beta\text{-}C_\alpha](10)+$ $\varphi[C_\delta\text{-}C_\gamma\text{-}C_\beta](6)$	111	—	—	$\tau[C_\gamma\text{-}C_\beta](21)+\tau[C{=}N](21)+\omega[N\text{-}H](18)$ $+\tau[C_\varepsilon\text{-}C_\delta](8)+\tau[C_\alpha\text{-}C](8)$
50	—	—	$\varphi[C_\beta\text{-}C_\alpha\text{-}C](28)+\varphi[C_\gamma\text{-}C_\beta\text{-}C_\alpha](21)$ $+\varphi[C_\delta\text{-}C_\gamma\text{-}C_\beta](13)+\varphi[C{=}N\text{-}C_\varepsilon](8)$ $+\varphi[C_\alpha\text{-}C{=}N](8)$	84	—	—	$\tau[C_\beta\text{-}C_\alpha](47)+\tau[N\text{-}C_\varepsilon](31)$
30	—	—	$\tau[C_\gamma\text{-}C_\beta](27)+\tau[C_\delta\text{-}C_\gamma](13)$ $+\tau[C_\varepsilon\text{-}C_\delta](12)+\tau[N\text{-}C_\varepsilon](11)+\omega[N\text{-}H](9)$	62	—	—	$\tau[C_\alpha\text{-}C](62)+\tau[C_\gamma\text{-}C_\beta](12)$ $+\tau[C_\delta\text{-}C_\gamma](10)$
20	—	—	$\tau[C_\alpha\text{-}C](31)+\tau[C_\beta\text{-}C_\alpha](26)$ $+\tau[C_\gamma\text{-}C_\beta](10)+\tau[C_\delta\text{-}C_\gamma](7)$	41	—	—	$\tau[C_\gamma\text{-}C_\beta](26)+\tau[C_\delta\text{-}C_\gamma](25)$ $+\tau[C_\beta\text{-}C_\alpha](18)+\tau[N\text{-}C_\varepsilon](11)$ $+\tau[C{=}N](7)+\tau[C_\varepsilon\text{-}C_\delta](6)$

Note: 1. All frequencies are in cm^{-1}.

2. *-observed frequencies are taken from work of Meada *et al.*, Ref. 14.

Methylene (CH_2) Group Modes

Several CH_2 groups appearing in the backbone of M-ε-PL chain make it possible to compare the CH_2 group modes of this polymer with those of Polyethylene (PE). The M-ε-PL molecule has four methylene groups that are flanked by the rigid (-$NH_2CHCONH$-) groups. This linear chain of CH_2 groups has selection rules different from those for an infinite chain. They are related to the dispersion of given normal mode of an infinite chain and the absorption/scattering occurs at the phase values given by the following relation

$$\delta = k\pi/(m+1) \tag{5}$$

Where m denotes the number of CH_2 groups in the linear chain linkage and $k = 1, 2 \ldots 4$. Thus the allowed values of δ for a given mode, would give rise to wave numbers on the corresponding dispersion curve for an infinite system which is polyethylene (PE)[25] in this case. The wave numbers thus obtained are given in Table V. The calculated CH_2 group frequencies of M-ε-PL are in good agreement with those calculated from the dispersion curves of PE [Figure 2]. Small

Table IV. Comparison of Amide Modes of M-ε-PL with other β-Sheet Polypeptides

	M-ε-PL		β-PLV		β-PALS		β-PG1		β-PLS	
Modes	$\delta = 0$	$\delta = \pi$	$\delta = 0$	$\delta = \pi$	$\delta = 0$	$\delta = \pi$	$\delta = 0$	$\delta = \pi$	$\delta = 0$	$\delta = \pi$
Amide A	3322	3335	3290	3290	3303	3303	3274	3274	3318	3318
Amide I	1639	1685	1638	1638	1640	1637	1642	1634	1637	1628
Amide II	1528	—	1545	1545	1521	1517	1520	1520	1532	1537
Amide III	1279	1291	1228	1228	1229	1217	1306	1287	1249	1270
Amide IV	549	538	548	684	600	—	630	711	533	773
Amide V	714	711	715	715	695	718	720	745	713	685
Amide VI	643	642	615	628	448	515	570	634	533	647

Note: 1. All frequencies are in cm^{-1}
2. PLV = Poly (L-Valine)[20]
PALS = Poly (O-Acetyl, L-Serine)[22]
PG1 = Polyglycine I[23]
PLS = Poly (L-Serine).[24]

Table V. Comparison of CH_2 modes of M-ε-PL with those from dispersion curves of Polyethylene (PE)

Modes	Calculated by selection rule from PE dispersion curves	M-ε-PL	
		Freq (calc.)	Freq (obs.) [Ref. 14]
CH_2 asymmetric stretch	2919*	2940,2935 2929,2925	2933^{R}, 2936^{IR}
CH_2 symmetric stretch	2848*	2858,2854, 2851,2848	2853^{R}, 2858^{IR}
CH_2 scissoring	1473	1460,1455	1461^{IR}
	1440	1442,1439	1440^{IR}
CH_2 wag	1386	1380	1376^{IR}
	1346	1345	1341^{IR}
	1286	1267	1264^{IR}
	1220	1235	1228^{IR}
CH_2 twist	1297	1267	1264^{IR}
	1292	1224	1228^{IR}
	1265	1201	1200^{R}
	1208	1166	1171^{IR}
	—	1150	1123^{IR}
	—	1120	—
CH_2 rock	992	961	956^{R}
	900	894	881^{IR}
	799	845	851^{R}
	743	811	831^{IR}
		734	730^{R}
C-C stretch	1054	1057	1064^{IR}
	1049	1027	1043^{IR}
	1028	995	1014^{IR}
	983	972	972^{IR}
		933	933^{R}

Note: 1. All wavenumbers are in cm^{-1}
2. *marked wavenumbers are observed in the spectra of polyethylene.

deviations could arise because of the intra and inter chain interactions of CH_2 group with (-NH_2CHCONH-) group in M-ε-PL.

Since the CH_2 groups in M-ε-PL are flanked by rigid (-NH_2CHCONH-) groups at both ends so due to such anchoring, a comparison of the wave numbers obtained from the dispersion curves of PE, corresponding to phase values given by equation (5) is in order in case of CH_2 group modes except for the skeletal modes. These modes in polyethylene mostly consist of coupled motions of φ(C-C-C) and τ(C-C) and

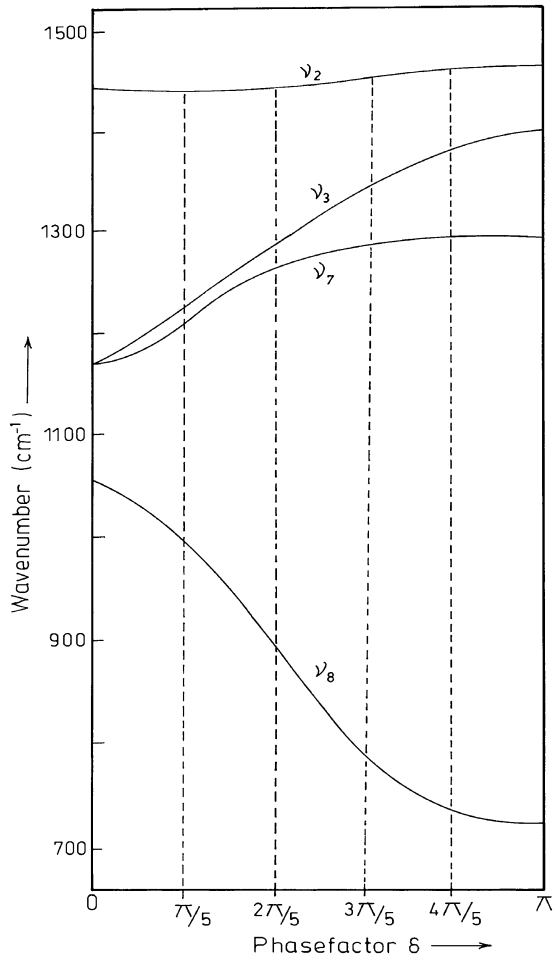

Figure 2. Dispersion curves of the scissoring (ν_2), wagging (ν_3), twisting (ν_7) and rocking (ν_8) modes of polyethylene. . . ., indicates the allowed phase values (δ).

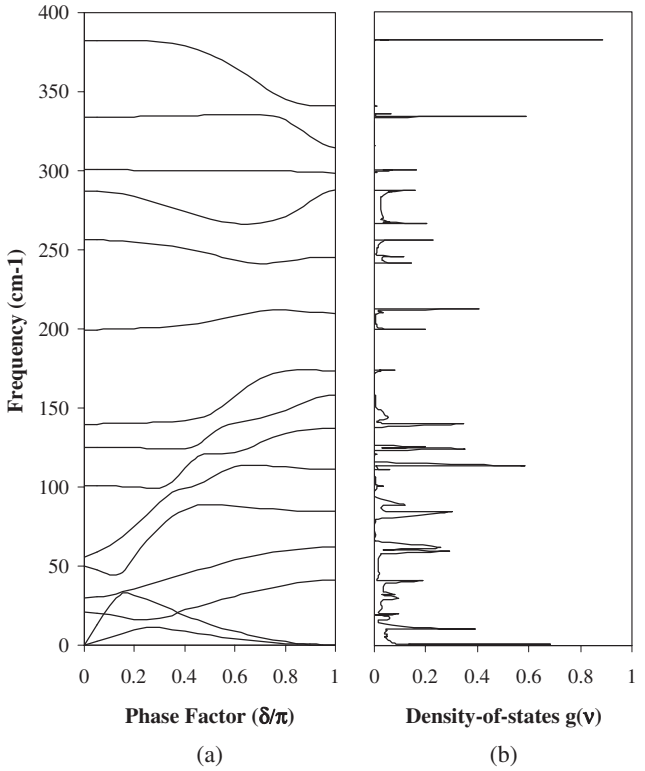

Figure 3. (a) Dispersion curves (Below 400 cm^{-1}). (b) Density-of-states (Below 400 cm^{-1}).

are spread over the entire chain. In PE, these modes are acoustical in nature whereas in M-ε-PL, the skeletal modes of (-CH_2-)$_4$ fragments are optical in nature and thus a comparison would not be in order. A similar phenomenon has been observed in nylon 6.[26–28] The origin of such optical phonon is explained by the splitting of the longitudinal acoustic phonon band of PE chain into several optical bands due to a periodic perturbation (the presence of the heavier amide groups -NHCO-). The same situation appears in poly(caprolactone) (PCL),[19] where CH_2 groups are flanked by (-COO-) groups.

Other Modes

The side group of M-ε-PL consists of an amino group and hydrogen attached to α-carbon. The NH_2 asymmetric and symmetric stretching modes calculated at 3417 and 3387 cm^{-1} are assigned to the observed IR peak at 3414(sh.) and 3386/3385 cm^{-1} (IR/Raman).[14] The same range of these modes is observed in case of poly(α-L-lysine)[16] [3420 & 3362 cm^{-1}].

The NH_2 group scissoring mode calculated at 1624 cm^{-1} is assigned to the observed peaks at 1639/1633 cm^{-1} (IR/Raman). Wagging mode of NH_2 group is calculated at 1401 cm^{-1}. This mode has also been observed at 1400 cm^{-1} in poly(α-L-lysine).[16]

The C_α-H stretching mode calculated at 2941 cm^{-1} is assigned to observed peak at 2936/2933 cm^{-1} (IR/Raman).[14] The C_α-H bending mode calculated at 1317 cm^{-1} matches well with observed peak at 1319 cm^{-1} (IR).[14]

Dispersion Curves

Dispersion curves and frequency distribution function are important for an understanding of thermodynamical and elastic properties of solids. Besides providing knowledge of density-of-states, dispersion curves give information on the extent to the coupling of a mode along the chain in the ordered state. Also a study of these is necessary to appreciate the origin of both symmetry independent and symmetry dependent spectral features. The dispersion curves and the corresponding density of states of M-ε-PL below 400 cm^{-1} are shown in Figure 3(a) and 3(b) respectively. Except a few, the modes above 400 cm^{-1} are almost non dispersive, hence not shown. The lower two branches ($\nu = 0$ at $\delta = 0$ & $\delta = \pi$) corresponds to four acoustic modes. Two of them are at the zone center and two are at the zone boundary. They represent three translations (one parallel and two perpendicular to the axis) and one free rotation about the chain axis.

The mode calculated at 382 cm^{-1} (at $\delta = 0$) remains undispersed upto $\delta = 0.40\pi$ but beyond this, the energy of this mode decreases continuously. At around $\delta = 0.75\pi$ mixing of PED of this mode with the lower mode at 334 cm^{-1} starts.

Beyond $\delta = 0.820\pi$, these modes move apart, showing repulsive feature. This repulsive feature between various modes is also observed in the dispersion curves of β-PALS, β-PLS etc. It is found that modes belonging to the same symmetry species repel one another.

The frequency of the mode calculated at 287 cm^{-1} at the zone centre decreases with δ and attains a minimum value at $\delta = 0.73\pi$. After this δ value its energy increases and the mode reaches 288 cm^{-1} at $\delta = \pi$. Contribution of $\varphi(C_\beta\text{-}C_\alpha\text{-}C)$ continuously decreases from the zone centre to the zone boundary. At the minimum point in this curve $d\omega/dk \rightarrow 0$, such critical points are known as Von-Hove type singularities in lattice dynamics. The two backbone torsional modes at 140 and 125 cm^{-1} at zone center move parallel upto $\delta = 0.42\pi$ but after this δ value, drastic increase in the energy takes place and they reach at 173 and 158 cm^{-1} respectively at $\delta = \pi$. A similar feature is found between the pair of modes at 125 and 100 cm^{-1}. The parallelism between two dispersion curves indicates that the speed of optical phonons is same in both modes.

The lowest optical mode crosses twice the upper acoustical mode at $\delta = 0.078\pi$ and $\delta = 0.376\pi$. The lower frequency modes, specially the acoustical modes are characteristic of the β-sheet polypeptides.

The two acoustical branches in the dispersion curves are similar in shape to the dispersion curves of these branches in Nylon 6,[28] PCL,[19] PG I,[22] poly(glycolic acid) (PGA).[29] The peaks in the acoustic curves of M-ε-PL occur at $\delta = 0.150\pi$ and $\delta = 0.275\pi$. A comparison with dispersion curves of Nylon 6[28] shows that the peaks in the acoustic curves fall at about the same δ value and the peak heights are nearly the same.

When the approaching modes belong to different symmetry species and polymeric chain has mirror plane symmetry then modes can crossover. Since M-ε-PL has a mirror plane of symmetry along the chain axis, hence crossings are permissible. A crossover implies two different species existing at the same frequency. They have been called as "non-fundamental resonances" which occur at a wave vector value away from the zone centre but within the zone boundary and as such their mode of vibration at this point can not be designated as a "normal mode." These are useful in the interpretation of the spectral features and interactions.

Frequency Distribution Function and Heat Capacity

The frequency distribution function as obtained from dispersion curves is shown in Figure 3(b). The observed frequencies compare well with the peak positions. The peaks in the dispersion curves correspond to the regions of high density-of-states and thus contribute to heat capacity. We have calculated the heat capacity of M-ε-PL in the temperature range (1–450 K) (Figure 4) using density-of-states *via* dispersion curves using Debye's formalism (eq 4).

Our calculations have been made for an isolated molecular chain, thus the interpretation of IR/Raman spectra and theoretical calculations are subject to certain limitations. A complete interpretation of the spectra requires calculations of dispersion curves for a three dimensional system which is a difficult job. Interchain modes involving hindered translatory and rotatory motion will appear and the total number of modes will depend on the contents of the unit cell. Apart from the large dimensionality of the problem, it would bring in an enormous number of interactions and make the problem somewhat interactable. The interchain interactions are generally of the same order of magnitude as the weaker intrachain interactions. They can affect the force constants and depending upon the crystal symmetry lead to the field splitting at zone center and zone boundary but the dominant assignments are unaffected. Thus in spite of these limitations, the present work provides a good starting point for further basic studies on the dynamic and thermodynamic behavior of polypeptides and proteins.

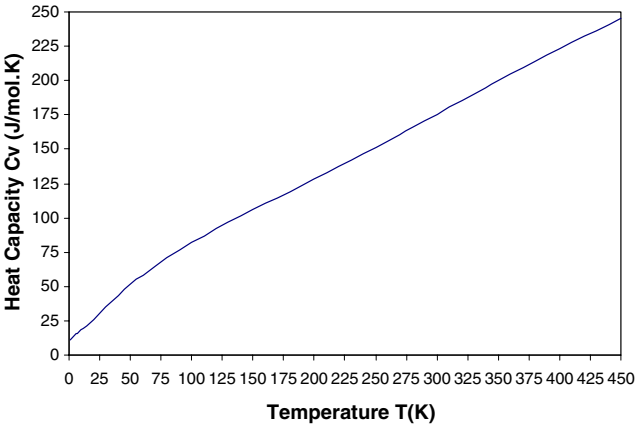

Figure 4. Variation of heat capacity with temperature (1–450 K).

CONCLUSION

All characteristic features of the dispersion curves such as regions of high density-of-states, crossing and repulsion between the various pairs of modes have been well interpreted from the vibrational dynamics of M-ε-PL. In addition, the predictive values of heat capacity as a function of temperature in the region 1 to 450 K are presented.

Acknowledgment. Financial assistance to one of us (M.S.) from University Grants Commission, New Delhi under faculty improvement programme (F.I.P.) is gratefully acknowledged.

Received: October 23, 2007
Accepted: February 10, 2008
Published: April 23, 2008

REFERENCES

1. F. Oppermann-Sanio and A. Steinbuchel, *Naturwissenschaften*, **89**, 11 (2002).
2. R. J. Gaymans and J. L. Hann, *Polymer*, **34**, 4360 (1993).
3. I. Arvanitoyannis, A. Nakayama, N. Kawasaki, and N. Yamamoto, *Polymer*, **36**, 857 (1995).

4. D. R. S. Kushwaha, K. B. Mathur, and D. Balasubramanian, *Biopolymers*, **19**, 219 (1980).
5. S. Shima and H. Sakai, *Agric. Biol. Chem.*, **41**, 1807 (1977).
6. S. Shima and H. Sakai, *Agric. Biol. Chem.*, **45**, 2497 (1981).
7. S. Shima and H. Sakai, *Agric. Biol. Chem.*, **45**, 2503 (1981).
8. S. Shima, Y. Fukuhara, and H. Sakai, *Agric. Biol. Chem.*, **46**, 1917 (1982).
9. Y. T. Ho, S. Ishizaki, and M. Tanaka, *Food Chem.*, **68**, 449 (2000).
10. I. L. Shih, M. H. Shen, and Y. T. Van, *Bioresour. Technol.*, **97**, 1148 (2006).
11. H. Lee, K. Oyama, J. Hiraki, M. Hatakeyama, Y. Kurokawa, and H. Morita, *Chem. Express*, **6**, 683 (1991).
12. H. Fukushi, K. Oyama, M. Hatakeyama, J. Hiraki, D. Fujimori, and H. Lee, *Chem. Express*, **8**, 745 (1993).
13. H. Lee, H. Yamaguchi, D. Fujimori, A. Nishida, and H. Yamamoto, *Spectrosc. Lett.*, **28**, 177 (1995).
14. S. Maeda, Ko-Ki Kunimoto, C. Sasaki, A. Kuwae, and K. K. Hanai, *J. Mol. Struct.*, **655**, 149 (2003).
15. S. Sasaki, T. Hishiyama, K. M. Huh, T. Ooya, and N. Yui, *Polym. Prep. Jpn.*, **50**, 2003 (2001).
16. N. K. Misra, D. Kapoor, P. Tandon, and V. D. Gupta, *Polym. J.*, **29**, 914 (1997).
17. E. B. Wilson, J. C. Decius, and P. C. Cross, "Molecular Vibrations: The theory of infrared and Raman vibrational spectra," Dover Publications, New York, 1980.
18. P. W. Higgs, *Proc. R. Soc. London*, **A220**, 472 (1953).
19. R. M. Misra, R. Agarwal, P. Tandon, and V. D. Gupta, *Eur. Polym. J.*, **40**, 1787 (2004).
20. L. Burman, P. Tandon, V. D. Gupta, S. Rastogi, and S. Srivastava, *Biopolymers*, **38**, 53 (1996).
21. N. K. Misra, D. Kapoor, P. Tandon, and V. D. Gupta, *Polymer*, **41**, 2095 (2000).
22. V. Porwal, R. M. Misra, P. Tandon, and V. D. Gupta, *Indian J. Biochem. Biophys.*, **41**, 34 (2004).
23. A. Gupta, P. Tandon, V. D. Gupta, and S. Rastogi, *Polymer*, **38**, 2389 (1997).
24. S. Krimm and J. Bandekar, *Adv. Protein Chem.*, **38**, 181 (1986).
25. M. Tasumi and T. Shimanouchi, *J. Mol. Spect.*, **9**, 261 (1962).
26. P. Papanek, J. E. Fischer, and N. S. Murthy, *Macromolecules*, **29**, 2253 (1996).
27. P. Papanek, J. E. Fischer, and N. S. Murthy, *Macromolecules*, **35**, 4175 (2002).
28. S. K. Shukla, N. Kumar, A. K. Mishra, P. Tandon, and V. D. Gupta, *Polym. J.*, **39**, 359 (2007).
29. R. Agarwal, R. M. Mishra, P. Tandon, and V. D. Gupta, *Polymer*, **45**, 5307 (2004).